

Lambda Scan for T- Channel Fermion Dark Matter

Emine GÜRPINAR GÜLER^{1*}

¹Konya Technical University, Faculty of Engineering and Natural Sciences, Department of Engineering Basic Sciences, Konya, Turkey
(ORCID: [0000-0002-6172-0285](https://orcid.org/0000-0002-6172-0285))



Keywords: Simplified Models, Large Hadron Collider, Dark Matter, Coupling Constant, t-channel Fermion Portal.

Abstract

The development of collider machines revealed a lot about matter in particle physics. The Large Hadron Collider (LHC) at CERN has made a great contribution to this field. Theorists proposed new models while comparing the LHC experimental data with the Standard Model (SM). Various parameters of many phenomenological studies have been tested for high-energy collisions. In this study, a simplified dark matter model, namely the t-channel Fermion Portal model, was examined with the lambda parameter scan at 14 TeV. Signal generation was performed using the Madgraph5 generator to scan the mediator and dark matter mass. The impact of the change in the lambda constant on the dark matter production mechanism of the model was investigated.

1. Introduction

One of the most exciting areas of particle physics is the study of dark matter. The link between dark matter (DM) and the Standard Model (SM) is the subject of the most investigations. Numerous cosmological and astrophysical observations provide strong support for the idea that dark matter exists. These are gravitational interactions. According to current measurements, the majority of dark matter acts like non-relativistic particles during structure development; they are commonly referred to as cold dark matter. These particles are stable throughout cosmic time scales, have no electrical charge, and are colorless. It should be noted, however, that certain models allow for the presence of hot, dark matter made up of relativistic particles. Today, dark matter makes up about 80% of the total density of matter in the universe. DM is investigated in three classes of search: (i) direct detection, which detects interactions of DM particles in terrestrial detectors [1-4], (ii) indirect detection, which detects DM-DM interactions in the cosmos, that is, DM-DM interactions at the center of the galaxy [4-8], and (iii) colliders, which produce DM and DM mediators in the Lab. The LHC at CERN is a

distinguishedly proper machine to look for DM particles. Those found through direct and indirect searches are supplemented by the most current constraints that were obtained from the CMS and ATLAS experiments conducted at the LHC. [9].

At a hadron collider, the signature of DM generation is an overabundance of events in which a single final-state particle X recoils against huge quantities of missing transverse momentum or energy (MET). Different "mono-X" signatures, where "X" might represent hadron or gauge boson jets, the Higgs boson, top or bottom quarks in the final state, etc., have been studied by the ATLAS and CMS teams at the LHC.

DM analysis is interpreted with various models that have been discussed at the LHC Dark Matter Working Group (LHC DM WG), which brings together theorists and experimentalists to define guidelines and recommendations for the benchmark models, interpretation, and characterization necessary for broad and systematic searches for dark matter at the LHC. One possible line that could shed light on this discussion is the use of simplified models [10]. Assuming a particle genesis for DM, it could be possible for it to interact with SM processes and common matter. The DM is

*Corresponding author: egguler@ktun.edu.tr

Received: 06.04.2023, Accepted: 21.03.2024

treated as a massive particle in simplified models, and its interactions with the SM are mediated by a particle called the mediator. The mediator is a color singlet that links to two particles of dark matter, or a standard model in the so-called s-channel model [11]. In contrast, the so-called t-channel simplified model postulates that the mediator only interacts with a single SM state and dark matter [12].

Here, we take a simplified version of the t-channel model into account, one in which dark matter fermions play a role. [13-15]. A detailed discussion of this model and its relevance for the monojet phase space can be found in Ref. [13]. This model was interpreted in monojet analysis with data collected between 2016 and 2018 in proton-proton collisions at 13 TeV in the CMS experiment and corresponds to an integrated luminosity of 35.9 [17] and 137 fb⁻¹ [18], respectively. In the case of the fermion portal model, the findings of the analysis were presented in the form of exclusion limits at a confidence level of 95% in the plane of the DM candidate mass M_χ and the mediator mass M_ϕ . It is assumed that the value of the coupling between the mediator, the right-handed up quark, and the DM candidate will remain unchanged and will be equal to $\lambda_u = 1$, and this is the default setting. In this study, we will show the result of the fermion portal model for 14 TeV at the parton level. First of all, we will determine the relationship between the lambda and the mediator, DM mass. Then we will show the signal cross-section expected for different signal hypotheses in the $M_\chi - M_\phi$ plane.

The following outline constitutes the structure of the current paper. In the next part, we will provide a concise definition of the framework for t-channel DM models, and then in the following section, the signal generation of our study will be discussed. In the fourth part, we present the findings and conclude.

2. T- channel Fermion Dark Matter Model

As stated in the previous section, the fermion portal DM model was compared with the proton-proton collision data obtained in the CMS experiment, and its limits were determined. For this reason, it is the most well-known of the t-channel models. Within the confines of this DM model [13], an SM singlet DM particle is responsible for mediating the interaction between quarks and the DM through a novel QCD color triplet state. As for the Lorentz properties of the DM model, there are several classifications of such models. One of these is the

Dirac fermion. Others are sorted as complex scalars, real scalars, Majorana fermions, or vectors. In this paper, our primary emphasis is placed on the scenario in which the DM is a spin-1/2 particle considered a Dirac fermion. Depending on the kind of quarks that the dark matter couples to, one may specify the dark matter in a variety of different ways. We assumed that Dirac fermion DM couples universally to righthanded quarks via a color-triplet scalar mediator. The mediator primarily couples with gluons because of its SU(3) color representation. The Lagrangian that describes the coupling of a color-triplet scalar to quarks is given as follows:

$$\mathcal{L}_\chi = \lambda_{u_i} \phi_{u_i} \bar{\chi}_L u_R^i + \lambda_{d_i} \phi_{d_i} \bar{\chi}_L d_R^i + \text{h.c.} \quad (1)$$

where $u_i = u, c, t$ ($d_i = d, s, b$) are different SM quarks, where ϕ is the DM mediator, where χ is the DM candidate, and where λ is coupling. The mediator's coupling with gluons can be represented by an effective Lagrangian term:

$$\mathcal{L}_{gluon} = \frac{\alpha_s}{\Lambda} \phi^\dagger T^a \phi G_{\mu\nu}^a \tilde{G}^{a\mu\nu} \quad (2)$$

where ϕ is the DM mediator, T^a are the Gell-Mann matrices, $G_{\mu\nu}^a$ is the gluon field strength tensor, α_s is the strong coupling constant, $\tilde{G}^{a\mu\nu}$ is the dual of the gluon field strength tensor and Λ is a cutoff scale.

For this analysis, we will presume that the branching ratio of the decay $\phi_{u_i} \rightarrow \chi \bar{u}^i$ is equal to 100 percent. The steps of the model's formation and degradation are depicted in Figure 1. For this investigation, we will only focus on the u quark; hence, our investigation of the three production methods in this study in the context of coupling to up quarks is depicted in Figure 1.

The generation of scalar mediator pairs is a task that is of the utmost significance to Hadron colliders. These scalar mediators eventually decay into Dark Matter (DM) particles and quarks as a result of their breakdown. As seen in Figure 1, this unique decay pattern has the potential to be a distinguishable experimental signature of FP DM models (a). The process for diagram (a) is denoted by the notation $pp \rightarrow \phi \phi \rightarrow \chi j \chi j$, and as a result, this phenomenon can be specifically defined by something that is referred to as the Two-phi mediator state. It is important to note that the final state of diagram (a) comprises two jets, which provides a unique

signature. In addition to that, there is an additional fascinating process for the manufacturing of the substance. Co-production between the DM candidate and the scalar mediator is possible, but only under certain circumstances. This mode of production leads to what is known as the One-phi mediator state, and the corresponding processes for Figure b are $pp \rightarrow \phi \rightarrow \chi\chi j$. This state has a mono-jet-like signature, as can be seen in diagram (b), which is one of the characteristics that sets it apart from diagrams (a) and (b).

The creation of paired DM candidates represents yet another potential route that could be taken with the production. This generation is accomplished by the utilization of a t-channel

exchange that incorporates the scalar mediator. It is not an easy task to implement this strategy with colliders. It is essential that parton radiation take place immediately from the ISR state, which is an abbreviation for the beginning state. Figure 1 illustrates this significant part of the manufacturing mechanism that is essential to its operation (c). The process that corresponds to Figure (c) is denoted by $pp \rightarrow \chi\chi j$. Because of the unique qualities that it possesses, this particular condition has been given the moniker of the mediator state of no-phi. This is an interesting fact. A mono-jet-like signature can also be seen in diagram (c), which is the same as diagram (b).

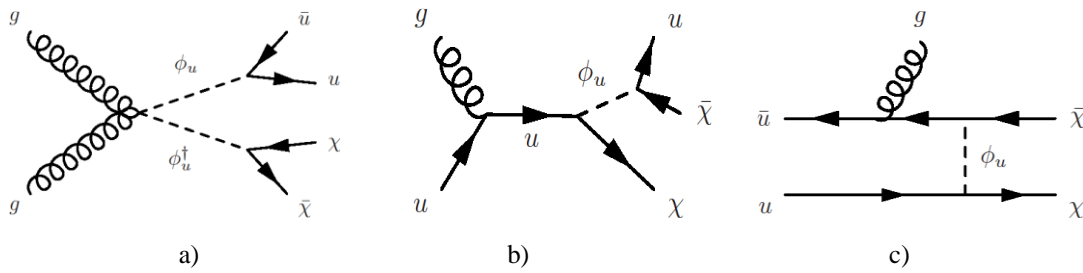


Figure 1. Feynman diagrams describe the creation procedures of Dirac fermions by DM particles in the FP model when they are produced at the LHC in combination with a single quark or gluon. The ultimate state of the diagram represented by (a) contains two jets. The process for diagram (a) is $pp \rightarrow \phi \phi \rightarrow \chi j \chi j$. The diagrams represented by (b) and (c) only have one jet each. The processes for diagram (b) and (c) are $pp \rightarrow \phi \rightarrow \chi\chi j$ and $pp \rightarrow \chi\chi j$ respectively [13]

3. Signal Sample Production

In this paper, we show the result of the FP Dirac DM model at the parton level. The FP signal is generated using the MadGraph5 generator [16] at 14 TeV. For each mass point were generated 10k events. For the sample generations, the couplings of the mediator with the SM and the DM particle have been considered for u quarks. In this model, a set of distinct parameters can be scanned to search for dark matter:

- Dark matter mass (M_χ)
- Mediator masses (M_ϕ)
- Coupling to SM particles (λ_u)

Benchmarks points are a set of (M_χ, M_ϕ) combinations with different couplings λ_u . The benchmarks consist of representative points to cover the most interesting kinematic features in phase space. To determine the cross sections for the model, the event rates for the collider production of the quark partners were calculated at parton level at leading order using MadGraph5 v2.6.6.

The MadGraph files were generated using Fermion portal model FeynRules. Figure 2 shows

signal cross-section expressed in pb, in the $M_\phi - M_\chi$ plane for $\lambda_u = 0.5, 1, \text{ and } 2$ a, b, and c, respectively, incorporating all processes seen in Fig. 1. ($pp \rightarrow \phi \phi \rightarrow \chi j \chi j$, $pp \rightarrow \phi \rightarrow \chi\chi j$ and $pp \rightarrow \chi\chi j$). It is clear seen that as the lambda increases, the cross section increases in the $M_\phi - M_\chi$ plane.

For the Dirac case, the decay width of the ϕ_u particle is determined as follows using the up quark operator [13].

$$\Gamma(\phi \rightarrow \chi + \bar{u}) = \frac{\lambda_u^2 (M_\phi^2 - M_\chi^2)^2}{16\pi (M_\phi^3)} \tag{3}$$

Figure 3 depicts the overall width in GeV as a function of M_ϕ and M_χ for coupling strength parameters λ_u 0.5, 1, and 2, respectively, incorporating all processes shown in Fig. 1. ($pp \rightarrow \phi \phi \rightarrow \chi j \chi j$, $pp \rightarrow \phi \rightarrow \chi\chi j$ and $pp \rightarrow \chi\chi j$). As can be seen clearly in equation 1, as the lambda increases, the width will increase proportionally to the square of the lambda.

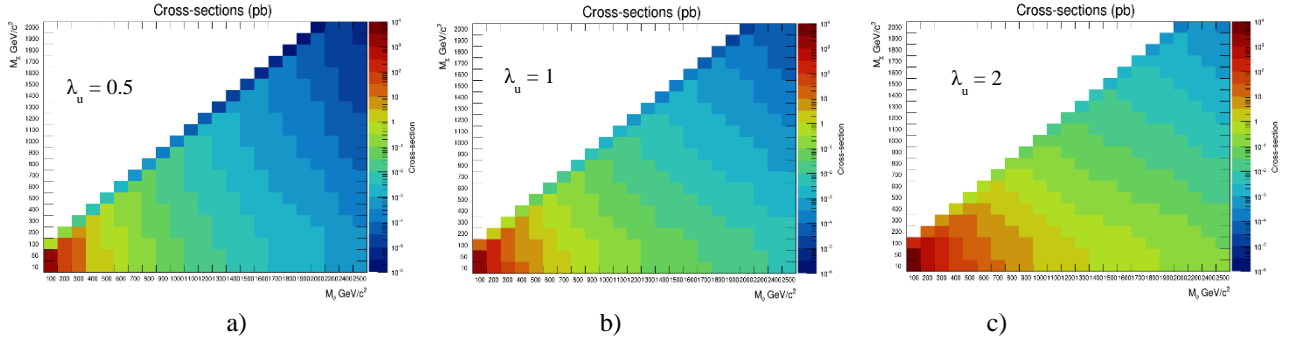


Figure 2. Signal cross-section expressed in pb, expected different signal hypothesis in the M_ϕ

- M_χ plane including all processes in Fig. 1. ($pp \rightarrow \phi \phi \rightarrow \chi j \chi j$, $pp \rightarrow \phi \rightarrow \chi \chi j$ and $pp \rightarrow \chi \chi j$) for $\lambda_u = 0.5, 1$ and 2 a, b and c respectively

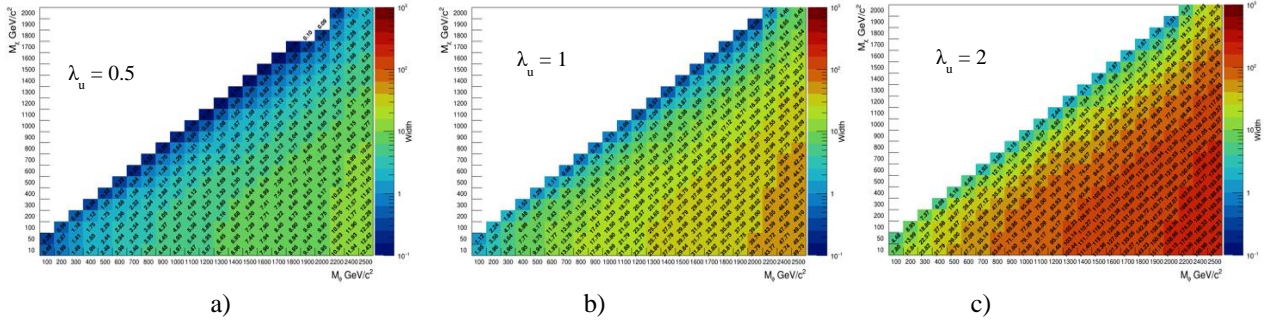


Figure 3. Total mediator width (ϕ) measured in GeV as a function of M_ϕ and M_χ including all processes in Fig. 1. ($pp \rightarrow \phi \phi \rightarrow \chi j \chi j$, $pp \rightarrow \phi \rightarrow \chi \chi j$ and $pp \rightarrow \chi \chi j$) for a) $\lambda_u = 0.5$, b) $\lambda_u = 1$ and c) $\lambda_u = 2$

The cross section for production is identical to that of a single squark when λ_u is close to 0 in the Minimal Supersymmetric Standard Model (MSSM), and the meaningful diagram that can produce it is (a) in Figure 1. In the scenario in which λ_u is not equal to zero, there are additional contributions from the t-channel dark matter exchange, and for the parton level process $u + \bar{u} \rightarrow \phi + \phi^*$, the cross-section is given by the following equation [13]:

$$\sigma = -\frac{1}{1728\pi s^3} \left\{ 2\sqrt{s(s-4m_\phi^2)} [4g_s^4(4m_\phi^2 - s) + 12g_s^2\lambda_u^2(s + 2m_\chi^2 - 2m_\phi^2) + 27\lambda_u^4 s] + 3\lambda_u^2 [16g_s^2(m_\chi^2 s + (m_\phi^2 - m_\chi^2)^2) + 9\lambda_u^2 s(s + 2m_\chi^2 - 2m_\phi^2)] \log \left[\frac{s - \sqrt{s(s-4m_\phi^2)} + 2m_\chi^2 - 2m_\phi^2}{s + \sqrt{s(s-4m_\phi^2)} + 2m_\chi^2 - 2m_\phi^2} \right] \right\} \quad (4)$$

Process (b) in Figure 1 is the most important contributor to the formation of monojets when u is

set to a low value. The equation that describes the resulting cross section at LO for $u + g \rightarrow \phi + \chi$ is as follows[13]:

$$\sigma(u + g \rightarrow \phi + \chi) = \frac{\lambda_u^2 g_s^2}{768\pi s^3} (3s + 2m_\chi^2 - 2m_\phi^2) \sqrt{(s + m_\chi^2 - m_\phi^2)^2 - 4m_\chi^2 s} \quad (5)$$

where \sqrt{s} is the center-of-mass energy.

4. Results and Discussions

This study was carried out to adjust the lambda constant to the most efficient monojet production of the signal to be produced for model interpretation of the data collected in proton-proton collisions with a center of mass energy of 14 TeV.

If $\lambda_u \approx 0$, jets plus missing transverse energy on pair production on a mediator that is in the diagram (Figure 1-a) gives the dominant

contribution. This can be seen in Figures 4c and 5c, where the production cross-section is bigger than Figures 4-a and 4-b or Figures 5a and 5b at $\lambda_u \approx 0$. It is the same as the search that is performed in the instance of supersymmetric (SUSY) models looking for squarks. In the event that the gluinos are

separated into individual particles, Squark interactions revolve around weak interactions in terms of their coupling. As a result, the significance of this contribution is minimal. The coupling, on the other hand, is a free parameter in the t-channel model, and it has the potential to be rather substantial

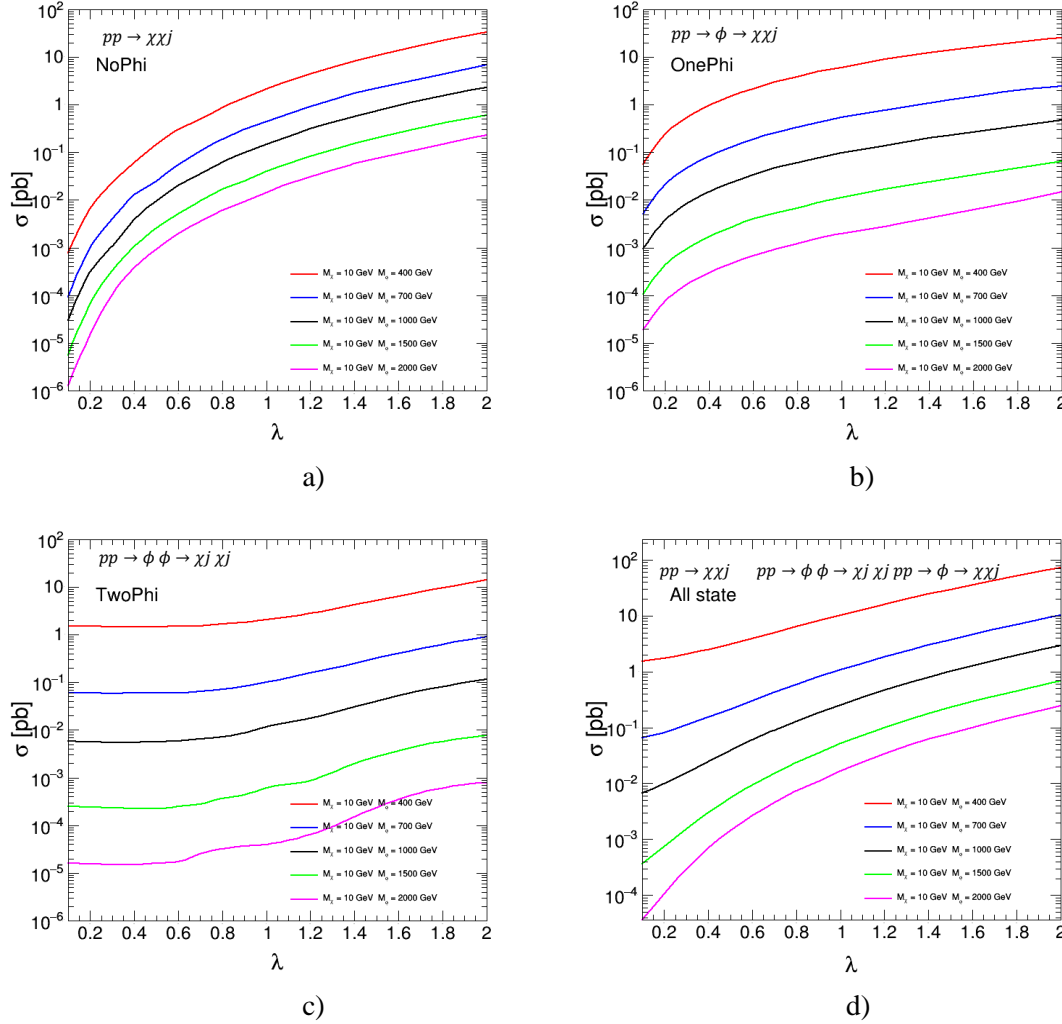


Figure 4. Production cross-section σ as a function of coupling λ_u for various mediator mass M_ϕ at fixed $M_\chi = 10$ GeV for no-phi mediator state ($pp \rightarrow \chi\chi j$) (a) one-phi mediator state ($pp \rightarrow \phi \rightarrow \chi\chi j$) (b) two-phi mediator state ($pp \rightarrow \phi\phi \rightarrow \chi j \chi j$) (c) and including all state ($pp \rightarrow \chi\chi j$ & $pp \rightarrow \phi \rightarrow \chi\chi j$ & $pp \rightarrow \phi\phi \rightarrow \chi j \chi j$) (d).

As expected, the t-channel DM exchange state and one mediator final state are dominant for $0.5 < \lambda_u < 2$, in a word, the monojet signature makes an important contribution to this search in this coupling range. The combination of production cross-section is reported in Figure 5, where the expected cross-section rate in pb is reported for several signal mass points in the M_ϕ - M_χ plane.

We observed that events with one phi state do not contribute to the cross-section when phi is

much larger than chi. This phenomenon is illustrated in Figure 5-b. There is no cross-section of the one ϕ state (Figure 1-a) when λ_u is greater than 2. Mediator pair production and t-channel production become the dominant contributors to the total cross-section state in this range. Since the production cross section decreases with decreasing coupling constants, the results, interpreted in terms of exclusion limit constraints, will be weaker for small coupling constants. Future searches,

particularly at colliders, need to cover a considerable allowable proportion of the parameter space for small couplings, even for the mediator masses that are lower than a few hundred GeV. It has also come to our attention that there is a destructive interference for λ_u in the range of 0.5 to 1.5 for two phi states, as is illustrated in Figure 4-c

and Figure 5-c for high M_ϕ and low M_χ . Consequently, we anticipate that the experimental limits from jets plus missing transverse energy on pair generation will weaken at some intermediate values of λ_u .

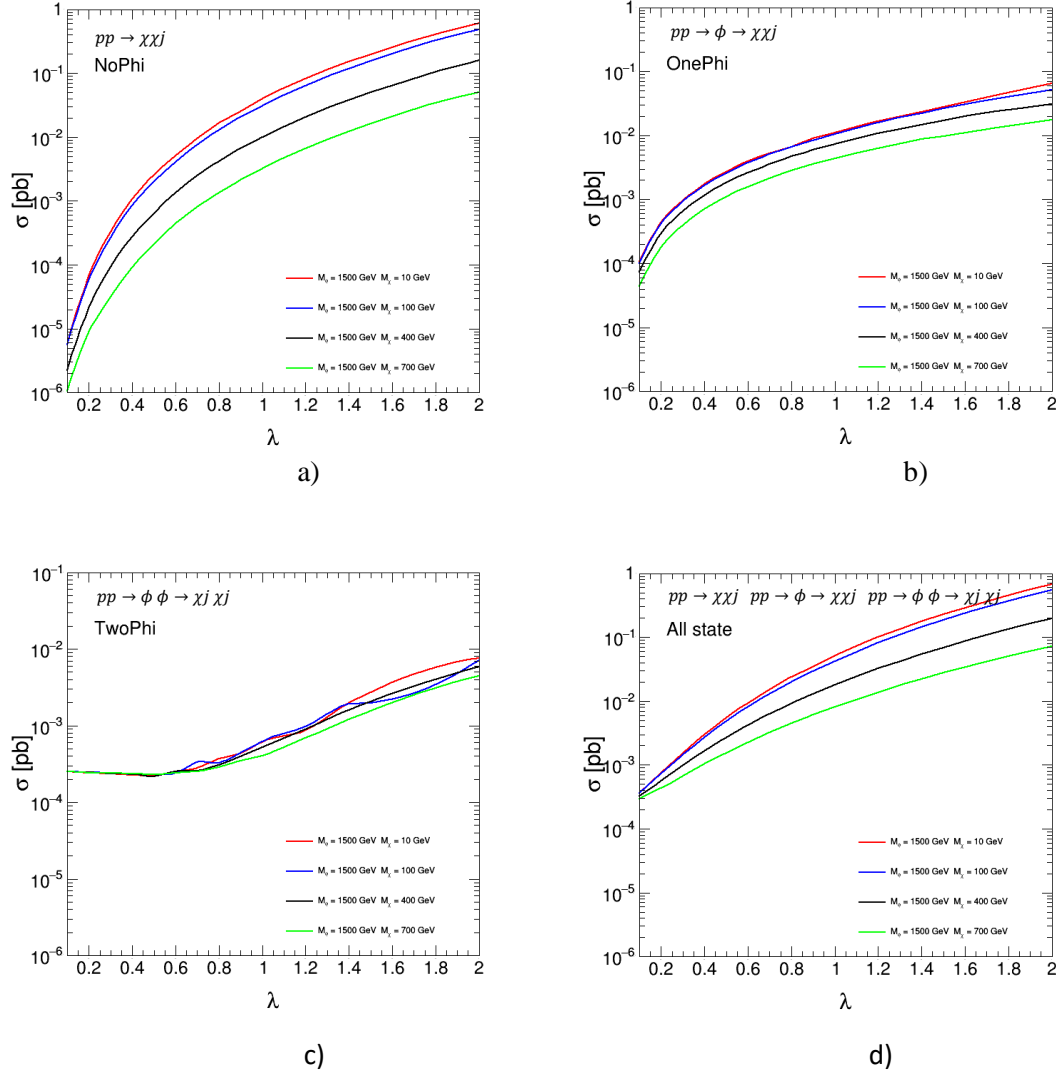


Figure 5. Production cross-section σ as a function of coupling λ_u for various mediator mass M_χ at fixed $M_\phi = 1500$ GeV for no-phi mediator state ($pp \rightarrow \chi\chi j$) (a), one-phi mediator state ($pp \rightarrow \phi \rightarrow \chi\chi j$) (b), two-phi mediator state ($pp \rightarrow \phi\phi \rightarrow \chi j \chi j$) (c), and including all state ($pp \rightarrow \chi\chi j$ & $pp \rightarrow \phi \rightarrow \chi\chi j$ & $pp \rightarrow \phi\phi \rightarrow \chi j \chi j$) (d)

5. Conclusion and Suggestions

Using a lambda parameter scan at 14 TeV, one of the simplified dark matter models, which is the t-channel Fermion Portal, is analyzed. The model's dark matter production mechanism was tested to see how it was affected by a change in the lambda constant. The T-channel Fermion Portal consists of three different

interaction processes, and the lambda sensitivity of these processes was examined separately. Our study exclusively focuses on the u quark, and as such, our exploration of the three production methods is contextualized within the framework of coupling to up quarks. Initially, differences in the cross-section in the M_χ and M_ϕ plane for different λ_u values, including all processes, were demonstrated. Then, the decay

width for the same λ_u in the M_ϕ , and M_χ plane was demonstrated, highlighting the lambda sensitivity of the model. Lastly, based on this data, the cross-section variation for different M_ϕ masses for a fixed M_χ mass as a function of λ_u values is separately shown for each process. Similarly, the lambda scan for each process is illustrated for different M_χ masses with a fixed M_ϕ mass. Based on the results presented in our paper, we can make the following observations: If λ_u is close to zero, the dominant contribution will be jets plus the missing transverse energy from pair production on a mediator. It is the same as the search that is conducted when supersymmetric (SUSY) models are used to look for squarks. λ_u Between a value of 0.5 and a value of 2, the t-channel DM exchange state and the one-mediator final state are the ones that clearly take the lead. However, when the value of phi is greater than that of chi, the contributions to the cross-section that come from events with a solitary phi state become substantially less important. When λ_u values are greater than 2, both the production of the mediator

pair and the production of the t-channel move into the foreground. Notably, the results of our research showed that there is a zone of destructive interference for λ_u ranging between 0.5 and 1.5 at particular mass points. This indicates that there may be a reduction in the size of the experimental boundaries. In light of these new discoveries, future experiments, particularly those based on colliders, will need to investigate a broad parameter domain in search of more subtle couplings. This is true even for mediators whose masses are lower than a few hundred GeV. This research sheds light on the critical parameters that guide monojet production and highlights the necessity of recalibrating experimental strategies in accordance with the λ_u spectrum.

Statement of Research and Publication Ethics

The study is complied with research and publication ethics.

References

- [1] D. S. Akerib, S. Alsum, H. M. Araújo, X. Bai, A. J. Bailey, J. Balajthy et al., "Results from a search for dark matter in the complete LUX exposure," *Phys. Rev. Lett.*, vol. 118, no. 2, p. 021303, 2017. [Online]. Available: arXiv:1608.07648, doi: 10.1103/PhysRevLett.118.021303.
- [2] E. Aprile et al., "First Dark Matter Search Results from the XENON1T Experiment," *Phys. Rev. Lett.*, vol. 119, no. 181301, 2017. doi: 10.1103/PhysRevLett.119.181301. [Online]. Available: arXiv:1705.06655
- [3] C. Amole, M. Ardid, I. J. Arnquist, D. M. Asner, D. Baxter, E. Behnke et al., "Dark Matter Search Results from the PICO-60 C3F8 Bubble Chamber," *Phys. Rev. Lett.*, vol. 118, no. 25, p. 251301, 2017, doi: 10.1103/PhysRevLett.118.251301. [Online]. Available: arXiv:1702.07666
- [4] M. Klasen, M. Pohl, and G. Sigl, "Indirect and direct search for dark matter," 2015. [Online]. Available: arXiv:1507.03800v1 [hep-ph] Jul. 14, 2015.
- [5] The Fermi-LAT, DES Collaborations, A. Albert, B. Anderson, K. Bechtol, A. Drlica-Wagner et al., "Searching for Dark Matter Annihilation in Recently Discovered Milky Way Satellites with Fermi-LAT," *Astrophys. J.*, vol. 834, no. 2, p. 110, 2017, doi: 10.3847/1538-4357/834/2/110. [Online]. Available: arXiv:1611.03184
- [6] M. Aguilar, L. Ali Cavazonza, B. Alpat, G. Ambrosi, L. Arruda, N. Attig, et al., "Antiproton flux, antiproton-to-proton flux ratio, and properties of elementary particle fluxes in primary cosmic rays measured with the Alpha Magnetic Spectrometer on the International Space Station," *Phys. Rev. Lett.*, vol. 117, p. 091103, 2016. doi: 10.1103/PhysRevLett.117.091103.
- [7] G. Ambrosi, Q. An, R. Asfandiyarov, P. Azzarello, P. Bernardini, B. Bertucci et al., "Direct detection of a break in the teraelectronvolt cosmic-ray spectrum of electrons and positrons," *Nature*, vol. 552, p. 63 EP, 2017. doi: 10.1038/nature24475.
- [8] M. G. Aartsen, R. Abbasi, Y. Abdou, M. Ackermann, J. Adams, J. A. Aguilar, et al., "IceCube Search for Dark Matter Annihilation in nearby Galaxies and Galaxy Clusters," *Phys. Rev. D*, vol. 88, no. 122001, 2013. [Online]. Available: arXiv:1307.3473. doi: 10.1103/PhysRevD.88.122001.
- [9] A. Albert, M. Backovic, A. Boveia, O. Buchmueller, G. Busoni, A. D. Roeck et al., "Recommendations of the LHC Dark Matter Working Group: Comparing LHC searches for heavy mediators of dark matter production in visible and invisible decay channels," 2017. [Online]. Available: arXiv:1703.05703.

- [10] D. Alves, N. Arkani-Hamed, S. Arora, Y. Bai, M. Baumgart, J. Berger et al., "Simplified Models for LHC New Physics Searches," 2011. [Online]. Available: <https://arxiv.org/abs/1105.2838>
- [11] A. Boveia, O. Buchmueller, G. Busoni, F. D'Eramo, A. D. Roeck, A. D. Simone, et al., "Recommendations on presenting LHC searches for missing transverse energy signals using simplified s-channel models of dark matter," 2019. doi: 10.1016/j.dark.2019.100365.
- [12] C. Arina, B. Fuks, L. Mantani, "A universal framework for t-channel dark matter models," *Eur. Phys. J. C*, vol. 80, 2020, Article no. 409. [Online]. Available: arXiv:2001.05024.
- [13] Y. Bai and J. Berger, "Fermion portal dark matter," *J. High Energy Phys.*, no. 11, Art. no. 171, 2013.
- [14] H. An, L. Wang, H. Zhang, "Dark matter with t-channel mediator: a simple step beyond contact interaction," arXiv:1308.0592v2 [hep-ph], Mar. 6, 2014.
- [15] C. Arina, B. Fuks, L. Mantani, H. Mies, L. Panizzi, J. Salko, "Closing in on t-channel simplified dark matter models," arXiv:2010.07559v2 [hep-ph], Dec. 31, 2020.
- [16] J. Alwall, M. Herquet, F. Maltoni, O. Mattelaer, T. Stelzer, "MadGraph 5: Going Beyond," arXiv:1106.0522 [hep-ph], [Online]. Available: <https://doi.org/10.48550/arXiv.1106.0522>.
- [17] The CMS Collaboration, A. Tumasyan, W. Adam, J. W. Andrejkovic, T. Bergauer, S. Chatterjee et al., "Search for new particles in events with energetic jets and large missing transverse momentum in proton-proton collisions at $\sqrt{s} = 13$ TeV," *J. High Energy Phys.*, vol. 2021, art. no. 153, 2021, doi: 10.1007/JHEP11(2021)153.
- [18] The CMS Collaboration, A. M. Sirunyan, A. Tumasyan, W. Adam, F. Ambrogi, E. Asilar, T. Bergauer, et al., "Search for new physics in final states with an energetic jet or a hadronically decaying W or Z boson and transverse momentum imbalance at $\sqrt{s} = 13$ TeV," *Phys. Rev. D*, vol. 97, no. 092005, May 2018. doi: 10.1103/PhysRevD.97.092005.